International Journal of Applied Pharmaceutics

ISSN- 0975-7058 Vol 15, Issue 4, 2023

Original Article

QBD APPROACH FOR THE DEVELOPMENT OF CAPSAICIN-LOADED GLYCYRRHETINIC ACID CONJUGATED STEARIC ACID GRAFTED CHITOSAN POLYMERIC MICELLES FOR ACTIVE HEPATIC TARGETING

MAYURI K.[1], SUNITHA S.[1*]

[1]Department of Pharmaceutics, Gitam School of Pharmacy, GITAM Deemed to be University, Hyderabad, Telangana-502329, India
[*]Corresponding author: Sunitha S.; [*]Email: ssampath@gitam.edu

Received: 08 Mar 2023, Revised and Accepted: 11 Apr 2023

ABSTRACT

Objective: Capsaicin (CAP) is a naturally occurring alkaloid forecasted in the treatment of Alcoholic Hepatitis (AH), but least studied due to its hydrophobicity, low bioavailability, and less target-specific release. Hence, the present study aimed to synthesize glycyrrhetinic acid conjugated stearic acid grafted chitosan (GA-CS-g-SA) and prepare CAP-loaded GA-CS-g-SA micelles.

Methods: Quality by design (QbD) approach in coordination with "Box-Behnken Designs (BBD)" was used to optimize the process parameters. GA-CS-g-SA was synthesized and characterized for its physic-chemical.

Results: The "Proton Nuclear Magnetic Resonance (^{1}H NMR)" spectrum depicted a strong signal at d=1.0 ppm and endorsed to-CH_2 group of SA and d=3.5-3.65 ppm depicting GA, which confirms the formation of GA-CS-g-SA. Critical micellar concentration (CMC) was found to be 13.45±1.72 µg/ml and amino groups substitute degree (SD %) was 10.12%±1.09%, indicating successful linkage of GA and SA on CS. The prominent peaks of CAP (0.9 and 1.31 ppm) in ^{1}H NMR spectra disappeared, indicating drug loading in the micellar core. Micelle's normal particle range was 167.54 nm, and encapsulation efficiency was 67.85%. The CAP-GA-CS-g-SA was found to be biocompatible following the hemolysis test. *In vitro* release pattern showed 78.68±3.12% in 24h, indicating the slower release of CAP from micelle, whereas 99.48±2.56% was released from non-micellar formulations in 6 h. CAP release from drug-loaded micelles showed a biphasic model with an early burst release in four hours, following a slower and sustained release pattern till 24h.

Conclusion: CAP-GA-CS-g-SA micelle is a hopeful advancement to progress bioavailability and controlled release of highly hydrophobic CAP. Further *in vivo* studies would be evident for targeting hepatocytes and treating AH using CAP-GA-CS-g-SA.

Keywords: Capsaicin, Chitosan, Stearic acid, Glycyrrhetinic acid, Micelles

DOI: https://dx.doi.org/10.22159/ijap.2023v15i4.47770. Journal homepage: https://innovareacademics.in/journals/index.php/ijap

INTRODUCTION

High alcohol intake is a significant risk factor counting many unfavorable health reactions such as Alcoholic Hepatitis (AH), causing morbidity and death [1].

Nearly one million cases of disability-adjusted life years (DALY) were reported in 2016 due to AH. Per head, alcohol utilization has inclined to 6.4 liters (2016) from 5.5 liters (2000). AH accounts for 34.3% patient population in India who suffer from liver-related diseases (2010). Alcoholic Liver Disease (ALD) by itself casts for 4% of the death rate and 5% of DALYs having European countries most affected. A million deaths were reported in 2010, accounting for fibrosis and cirrhosis concerning alcohol; among ten, one death is attributed to AH [2]. In the US population, a death rate of 5.5 per 100,000 was anticipated in 2010. AH is linked to 41% of the death rate in the European Union [3]. Having considerable advances in the ground of AH treatment, the existing treatment strategies have huge limitations; no impact on survival (Glucocorticoids), increased infection frequency within two months (Anti-TNF therapy), unsuccessful in treating (caspase inhibitors, probiotics), and reversal with increased seriousness making the treatment difficult [4].

To overcome the adverse events and improve the epidemiology of AH, it is necessary to treat the life-threatening disease. In recent studies, alkaloids have shown clinical advancement, majorly Capsaicin (CAP) of capsicum species have been under examination for their wide variety of pharmacological applications like anti-inflammatory [5], anti-obesity, antioxidation [6], anti-carcinogenic, and lowering of lipid peroxidation [7].

Although it has an extensive spectrum of beneficial possibilities, it is unexplored because of its limitations, such as low oral bioavailability, hydrophobicity, gastric irritation, burning diarrhea, nausea, and vomiting [8]. Hence it is necessary to explore a formulation strategy to reduce the complications and increase the oral bioavailability of CAP.

Chitosan (CS), a natural polysaccharide, has outstanding hydrophobicity, blood compatibility, bio-performance, and microbial decadence properties, well recognized for various biomedical functions such as controlled delivery of hydrophobic drugs [9]. Molecular weight (5 kDa), high viscous nature, less solubility in biological fluids (pH 6.3 to 7.8), and low cell specificity have restricted the use of CS *in vivo* [10]. Chemical alteration of CS was a capable approach to confiscate the limitations, resulting in improved transfection effectiveness and targeting capacity.

In recent years, many studies have been carried out to use hydrophobic longer-chain fatty acid of SA to graft CS to form CS-grafted-SA (CS-g-SA). Further, it self-aggregates to make polymeric micelles in an aqueous solution [10]. Additional studies found that CS-g-SA micelles had a spatial organization with a multi-hydrophobic core [11].

CAP-loaded CS-g-SA (CAP-CS-g-SA) distributes uniformly in blood circulation yet has a relatively low concentration in the hepatic cells, causing a less therapeutic outcome. At the same time, the other vital organs are affected by the harmful properties of the medicines acting against AH.

Liver targeting deliveries could release drugs effectively by reducing systemic circulation, dosage reduction, and rate of administration, further benefiting the therapeutic index and diminishing the adverse reactions associated [12]. Hepatocytes contain various receptors (Asialoglycoprotein receptor, Glycyrrhetinic acid receptors, IgA-Receptors, Transferrin receptors, HDL receptors, LDL receptors, Insulin receptors, and Scavenger receptors) on the surface, which can be accommodated for targeting the liver [12]. The receptors attach various ligands that can be formulated for the active targeting of the drug. Various studies show that glycyrrhetinic acid (GA)

receptors have been the popular option for targeting the hepatocytes affected by AH and can identify the GA ligand [13]. For the development of target delivery, a carrier that improves efficiency and has sufficient physiological security is much needed; CS-g-SA is a carrier that has been attached to GA and performs active release of CAP [14].

The diagrammatic representation is presented in fig. 1.

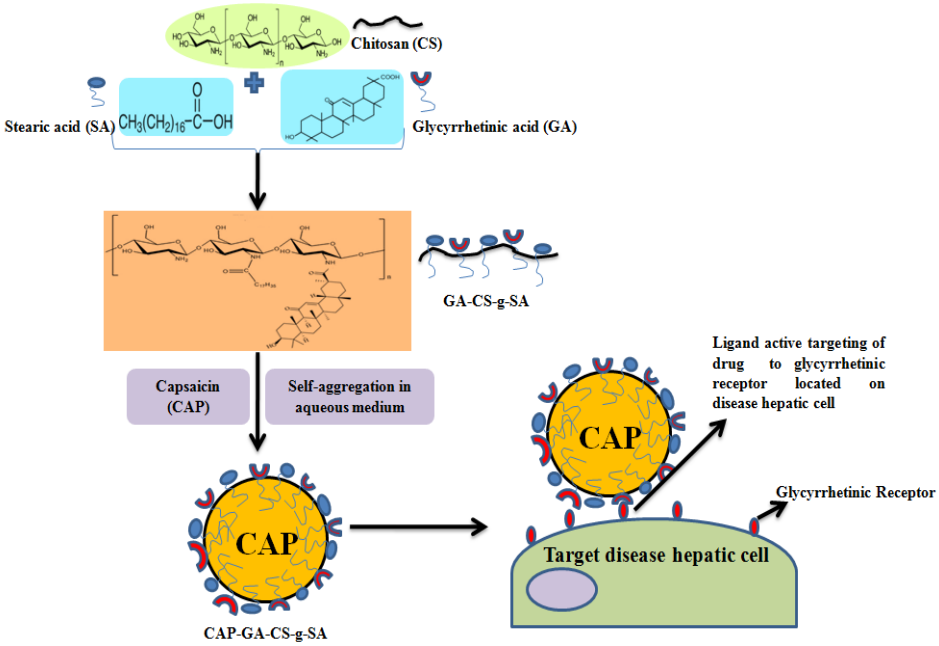

Fig. 1: Formation and ligand active targeting of drug to diseased cell

Utilizing "Design of Experiments (DoE)" is an innovative advance in the optimization and transmission of experimental factors. Simple experimental plans and statistical tools for information analysis can offer a huge advantage regarding the system under examination after a small number of experiments [15]. "Response Surface Methodology (RSM)", is a statistical method used for DoE and the construction of experimental models linking many interactive parameters [16]. "Box–Behnken Design (BBD)" is used for response surface modeling.

The current study aims to synthesize glycyrrhetinic acid-conjugated stearic acid-grafted chitosan (GA-CS-g-SA) using DoE. Study includes process optimization, preparation, and evaluation of the polymeric micelles of GA-CS-g-SA with CAP loaded (CAP-GA-CS-g-SA) [17] to increase the oral bioavailability and release the drug at inflamed hepatic cells in order to treat the AH.

MATERIALS AND METHODS

Capsaicin is obtained from AOS Products Private Limited, Ghaziabad. CS, oligosaccharide with M. Wt. of 5 kDa and degree of deacetylation of 85% and dialysis membrane (3kDa) obtained from Himedia Laboratories Pvt Ltd., Mumbai, India, SA, 1-ethyl-3-(3-dimethyl aminopropyl) carbodiimide (EDC, ≈ Purity%), N -hydroxysuccinimide (NHS, purity≈ 98%), 2,4,6 -trinitrobenzene sulfonic acid (TNBS), 1-dodecyl-pyridinium chloride (DPC with purity ≈ 98%), glycyrrhetinic acid were obtained from Sigma Aldrich, New Delhi, Dimethyl sulfoxide, ethanol, sodium bicarbonate, hydrochloric acid, Iodine, Potassium Iodide, obtained from SD Fine chemicals, Hyderabad, Millipore, filter paper-0.45 µm (M/s Merck Specialities Pvt. Ltd., Mumbai, India).

Design of experiments

Quality by design (QbD) for product development

QbD is a methodical proposition for improving the product with pre-established targets that include previous knowledge, DoE, assessment of possibility, and understanding through the product's life cycle. The QbD integrates quality during formulation development, contrasting conventional methods (quality analyzed after production) [18]. QbD comprises forming the superior grade targeted product outline and identifying the major quality features, vital material characteristics, and significant method parameters. In the current work, QbD was conducted as per the steps mentioned:

i. Risk review (relationship of cause and effect) for recognizing associated criteria that affect CQAs.

ii. Testing the variables

iii. Optimization and embarking on design space

QTPP and CQAs

QTPP comprises a probable outline of preferred features of an end product to ensure product quality, safety, and efficiency. Recognizing QTPP is the initial step in QbD, followed by the recognition of CQAs [19].

Risk assessment deals with analyzing various factors concerning the final CQAs. In addition, factors significantly affecting the CQAs have to be recognized [20].

GA-CS-g-SA synthesis

The GA-CS-g-SA be synthesized as per a method reported with slight modification [21]. Briefly, molar ratio 0.001: 0.0003 of CS and SA (CS 500 µg and SA~ 95 mg) were dissolved in 20 ml of dimethyl sulfoxide (DMSO). GA (50 mg) dissolved in DMSO (2.5 ml) was added dropwise to the above solution. The resultant solution was sonicated (Sonics and Materials, Inc., Vibra cell VCX 750) for 15 min at 50°C, further SA was stimulated by 1-ethyl-3-(3-dimethyl-aminopropyl) carbodiimide (EDC-50µg) in the presence of N-hydroxy succinimide (NHS-0.06µg), and the reaction was carried out in a hot water bath (50 °C for 30 min) at 1000 rpm. The reaction mixture is maintained at 50 °C for 12 h to complete the reaction. The blend has brought to room temperature and stirred continuously for 24 h at 2000 rpm. Dialysis (dialysis membrane-MWCO, 3.5 kDa) was performed for 72 h using water to eliminate the by-products. The mixture was dried in an oven, and the precipitate was extracted from the suspension by transferring it through a 0.45 m Millipore filter. The precipitate was harvested and used for further studies [22].

Characterization of GA-CS-g-SA

Amino groups substitute degree–GA-SA-g-CS (SD%)

The "2-4-6-trinitrobenzene sulfonic acid (TNBS)" technique was used to calculate SD% [11]. The measured volume of NaHCO3 (4%) and 0.1% TNBS (0.1%) were added sequentially to different CS and GA-CS-g-SA solutions concentrations and incubated (37°C for 2 h), followed by the adding 2 mol/l HCL. Absorbance was deliberated at 344 nm by ultraviolet-visible spectrophotometry (Shimadzu SPD-10A, Japan) after 30 min ultrasonication [23].

Critical micelle concentration (CMC)

Iodine method was used to determine the GA-CS-g-SA's CMC. The dilutions of GA-CS-g-SA were prepared (1.0 µg/ml-1.0×103 µg/ml) and sonicated (30 min) at room temperature [24]. UV absorbance was determined at 366 nm, and a plot was drawn between the intensity of adsorption and micelle concentration. The pointed enlargement in the absorption of the plotted graph indicates the CMC [11].

Preparation of micelle by active drug loading

Micelle was initially prepared by dissolving GA-CS-g-SA of 200 mg in ultrapure water (200 ml) under sonication (Sonics and Materials, Inc., Vibra cell VCX 750) in an ice bath for 30 min for 20 cycles (400 W, pulse on for 2.0 and off for 3.0 s) [25]. The CAP solution was dropped into the empty micelle solution while being constantly stirred [26]. The CAP-filled micelles were transferred into a dialysis container (MWCO, 3.5 kDa) with 10 vol. of ultrapure distilled water. Distilled water was substituted every 30 min to remove the free drug and DMSO. Finally, CAP-GA-CS-g-SA micelle was obtained in the dialysis bags and lyophilized using a freeze-dryer ("-80 °C and 10 mm Hg, Freezone 6liter, Labconco Corporation, Kansas City, MO,US) micelles were used for further study [11].

Optimization of process parameters for the preparation of micelles using BBD

The effects of three controlled variables—dialysis duration (A), the volumetric ratio of organic to water phase (B), and stirring time (C)—on two response variables—encapsulation efficiency (EE) and particle size of CAP-loaded micelles—were investigated using the Response Surface Methodology with BBD [27]. The BBD got engaged to develop and examine main, interactive, and quadratic effects following variables influencing resultant parameters [28]. Seventeen experiments were produced by "Design-Expert® 11.0 (Stat-Ease Inc., Minneapolis, Minnesota, USA)" [23]. Conditions following experiments due to the trials are furnished in table 1.

Table 1: List of dependent and independent variables

Screening of significant factors for the preparation of micelles using BBD					
Autonomous criteria			**Magnitude**		
Criteria		**Units**	**Low**	**Intermediate**	**High**
A	Dialysis time	min	60	120	180
B	Organic: Aqueous phase	v/v	1	2	3
C	Stirring time	min	30	60	90
Reliantriteria			Objective		
Y1	Encapsulation efficiency	%	Increase		
Y2	Particle size	nm	Decrease		

Characterization and evaluation of micelles

Encapsulation efficiency (EE)

The EE of CAP in the micellar system was determined by a filtration process [29]. CAP-GA-CS-g-SA micelle (5 mg/ml) was diluted using distilled water and filtered with a 0.22 µm filter membrane to eliminate non-encapsulated CAP. Later, 0.1 ml filtrate was carefully mixed with the pure chromatographic methanol to get a volume of 10 ml. The amount of encapsulated CAP was determined using UV–Vis spectrophotometer at 281.12 nm. The following equation can express the EE % calculations of CAP-GA-CS-g-SA micelle [30].

$$\text{Encapsulation efficiency (\%)} = \frac{\text{Amount of drug after filtration}}{\text{Total amount of drug in the sample}} \text{X } 100$$

Particle size, zeta potential, and polydispersity index

Particle size distribution of blank micelles and CAP-GA-CS-g-SA micelles was evaluated by dynamic light scattering method using a Malvern particle size analyzer (Master sizer 2000, Malvern, UK). For zeta potential, diluted micelles dispersions were placed in polystyrene electrophoretic cells. The micelles' zeta potential was evaluated using an "Au-plated electrode (U shape)" cell for a count of up to 250 particles per sec at 25 °C. Experiments were repeated thrice [31].

Surface morphology by transmission electron microscopy (TEM)

The morphology of CAP, blank micelles, and CAP-GA-CS-g-SA micelles was monitored using "TEM JEM 2100 (JOEL, Tokyo, Japan)". Micelle was placed on top of a film-coated Cu grid, marked by 2% (w/v) "phosphotungstic acid" solution, and, allowed to dry meant for contrast enrichment. Samples were analyzed at 45000× intensification using transmission electron microscopy [32].

^{1}H nuclear magnetic resonance (^{1}H NMR)

^{1}H NMR spectrum was used to confirm the synthesis of the GA-CS-g-SA and for the analysis of CAP-GA-CS-g-SA micelles. ^{1}H NMR spectra for drug, polymer, unloaded polymeric micelle and drug-loaded micelles (CAP, CS, GA-CS-g-SA, SA, and CAP-GA-CS-g-SA) were established (Varian Unity-Plus 400 NMR Spectrometer in $CDCl_3$) to verify the formation of GA-CA-g-SA [30].

Fourier transmission infrared spectroscopy (FTIR)

The FTIR spectra of CAP, CS, SA, GA-CS-g-SA, and CAP-GA-SA-g-CS were obtained utilizing KBr (Potassium Bromide) disc process (Tensor 27, FT-IR Spectrophotometer) with a range of 4000-600 cm^{-1}.

X-ray diffraction pattern

The "X-ray diffraction pattern" of CAP and CAP-GA-SA-g-CS was reported using a "Philips X-ray diffractometer (PW-1710)" operated using graphite monochromator, with operating circumstances, "Ni filtered Cu Kα radiation, 30 kV voltage, 20 mA current, and scan speed 1 °2θ min^{-1}"[33].

Differential scanning calorimetry

Thermal analysis of CAP and CAP-GA-SA-g-CS was performed using Perkin Elmer STA 8000 Thermal Analyzer. Calibrated (using indium) instrument was utilized in favor of the melting point and heat of fusion. A rate of 10°C/min got engaged in an array of 30-400°C. Regular Al (aluminum) sampling pans (Perkin-Elmer) were used; a vacant pan was placed as a reference. A triplicate examination was conducted on samples (5 mg) using nitrogen purge [34].

Hemolysis test

A hemolysis study was performed by isolating erythrocytes from human blood (heparinized) using centrifugation (2,800 rpm, 5 min). The established erythrocyte lump was re-suspended in PBS-phosphate buffer saline (pH 7.4). These washing steps have to be repetitive (thrice). Separated erythrocytes were re-suspended in 0.9% NaCl to get 2% (v/v) of erythrocyte suspension [35]. The suspension (1.8 ml) was then incubated with 0.2 ml of test specimens for 30 min at 37 °C and centrifuged (2,800 rpm, 5 min). Percent hemolysis of supernatant was calculated using a UV–Vis spectrophotometer at 545 nm. The PBS (pH 7.4) was used as a negative control having no hemolysis and distilled water as a positive control (100% hemolysis). The hemolysis percentage was determined with the equation [36].

$$\% \text{ Hemolysis} = \frac{\text{ABS}_{\text{Sample}} - \text{ABS}_0}{\text{ABS}_{100} - \text{ABS}_0} \text{X } 100$$

Where ABS_0-Absorbance-0% hemolysis

ABS_{100}-Absorbance-100 % hemolysis

***In vitro* drug release**

In vitro CAP release from micelles was performed *via* dialysis [37]. Before the day of the study, the dialysis bags were soaked in distilled water for overnight. The dialysis bags were filled with free CAP and CAP-GA-SA-g-CS (10 mg). The dialysis bags were hung in 100 ml PBS-capable containers that served as the release medium (pH 7.4,). Containers were swirled at a rate of 300 rpm/min at 37 °C. A release medium (5 ml) was drawn at each time point. An equal measure of the clean medium was refilled to preserve sink conditions. CAP concentration in the release medium was estimated, and the accumulative release percentage of CAP was calculated [29]. The experiment was conducted in triplicates.

Drug release kinetics

The drug release method and its approach from *the in vitro* release study were confirmed by integrating it into kinetic models (0 order, 1st order, Higuchi's, and Korsemeyer Peppa's model). The fitting curve technique understood CAP release through micelle formulation [38]. Results obtained through *in vitro* release studies were verified with different kinetic equations [39].

Stability of micelles

The stability of CAP-GA-CS-g-SA micelles was evaluated at different temperatures (4, 25, and 40 °C) for three months. Content of CAP, EE, mean PS and topography of drug-loaded micelles was established on the 1st, 15th, 30th, 45th, 60th, and 90th d [40].

Table 2: Kinetic equations

Zero order model	First order model	Higuchi model	Korsmeyer–peppas model
$Q_t = Q_0 + K_0 t$	$l\,n(Q_\infty - Q_t) = lnQ_0 + Kt$	$Q_t = k_H t^{\frac{1}{2}}$	$\frac{Q_t}{Q_\infty} = K_K t^n$
Q_t-Quantity of drug dissolved in time t, Q_0-Original quantity of drug K_0-Zero order release constant.	Q_t-Quantity of drug dissolved in time t, Q_0-Original quantity of drug Q_∞-Amount released in time ∞ (100 % drug release) K-First order release constant.	Q_t-Quantity of drug dissolved in time t, k_H-Higuchi dissolution constant.	Q_t-Amount of drug dissolved in time t, Q_∞-Amount released in time ∞, K_k-Rate constant n-Diffusional exponent

Statistical analysis

Results were articulated as mean±SEM, n=3. Statistical analysis is done by one-way ANOVA, which is followed by Dunnett's multiple comparison tests. Results were computed for statistical analysis using Origin pro (V 8.0). The value $p<0.01$ was regarded as statistically considerable.

RESULTS AND DISCUSSION

Design of experiments

Quality by design (QbD) for product development (QTPP and CQAs)

This study objective was to organize GA-CS-g-SA (ligand-carrier system) for hepatocyte intake and to improve oral bioavailability (CAP). Recognizing CQAs is an initial step in the QbD method and the organization of CQAs in the accepted range ensures the attainment of QTPP [41]. EE and particle size (Micelle formulation of CAP-GA-CS-g-SA) have opted as CQAs (table 3). Size affects the cellular uptake where minor particles have enhanced penetration and size reductions confer drug availability in a dispersed form, enhancing the dissolution. The EE is the quantity of drug that is included in the micelles. Elevated EE is desired to have advantages [42].

Risk estimation and recognition of CMAs and CPPs

Early assessment of risk factors was initiated by preparing an Ishikawa (fishbone) drawing (fig. 2). It depicts the result of each parameter on the CQAs. Amongst various factors, the influential factors were measured for test trials [43].

Synthesis-GA-CS-g-SA

The GA-CS-g-SA was synthesized through amidation among–NH_2 groups of CS and–COOH functional groups of SA and GA in the presence of EDC ("cross-linking pairing agent") along with NHS [23]. The -COOH of SA and GA gets reacted with EDC to form unstable intermediates ("-OO-acyl isourea derivative"). The formed intermediates reacted further with EDC to make active esters [24]. Finally, the active esters counter with 1° amino group of CS to structure amide bonds (amidation) to generate CS-g-SA [4]. Synthesis of GA-CS-g-SA was confirmed by ^{1}HNMR.

Characterization of GA-CS-g-SA (CMC and SD%)

Self-assembled amphiphilic micelle depicts a low CMC and is beneficial for intactness. The lower CMC values show a higher tendency to form micelle [23]. The CMC value of GA-SA-g-CS was about 13.45±1.72 µg/ml, lower than low molecular weight surfactants in water [36]. UV absorbance was determined at 366 nm (KI/I_2 standard solution), and a plot was drawn between the absorbance and GA-CS-g-SA micelle concentration. The "pointed peak" in the absorbance of the graph indicates the CMC (fig. 3).

Substitution degree % of GA-CS-g-SA is the proportion of SA substituted–NH_2 groups on CS. TNBS reacts with open–NH_2 groups on CS and forms trinitrobenzene associates having UV absorption at 344 nm. SD% of GA-CS-g-SA was 10.12%±1.09%, indicating the successful linkage of GA and SA on CS [44].

Table 3: QTPP and CQAs identification

QTPP	Target	Justification
Formulation	Nanosized Micelles	Polymeric micelles have emerged as potential nanocarriers for delivering difficult-to-formulate active moieties with enhanced bio-availability, reduced toxicity, extended-release, long circulation, and specific targeted delivery.
Administration mode	Oral	The merchandised product is oral; hence intention is to improve the oral bio-availability.
Pharmacokinetics	To improve	For increased bioavailability
Stability	No evident indication of aggregation after 30 d of preparation	The efficiency of the preparation relies on particle size; thus, it is significant to preserve without much variation
CQA	Aim	Rationalization
Particle size	Average particle size below 200 nm	Nano-scale size enhances surface area to enhance solubility and dissolution, which results in bioavailability improvement and reduction in pharmacokinetic variation.
Encapsulation efficiency (EE)	Superior	Superior EE ensures increased drug loading

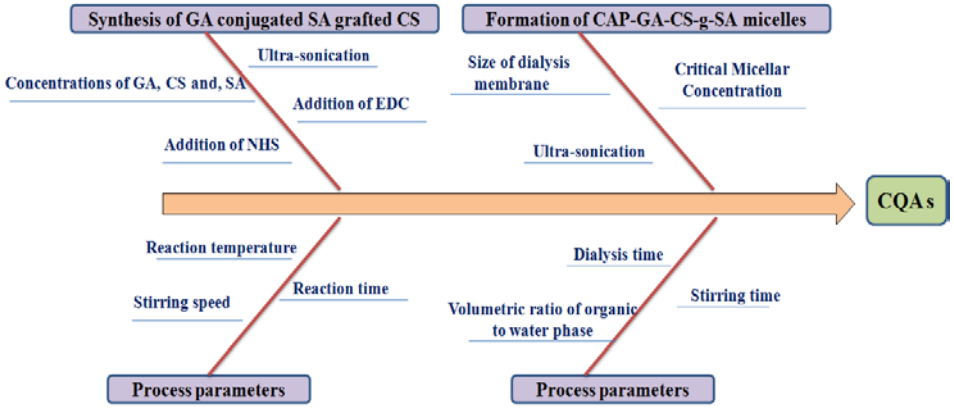

Fig. 2: Ishikawa (Fishbone) diagram showing cause and effect relationship for the production of CAP-GA-CS-g-SA

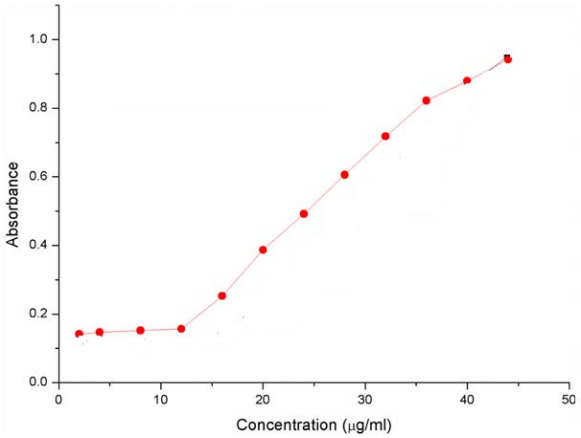

Fig. 3: Graph for determination of CMC value

Preparation of micelle by active drug loading

The synthesized GA-CS-g-SA was placed in distilled water with ultrasonic; initially, the empty micelles were formed due to their inherent self-aggregation behavior in an aqueous environment. The drug was stably entrapped in the core of the micelles by active loading and resulted in nano-sized micelles [40].

Optimization of process variables in the formation of micelles

A set of seventeen experiments was performed with a three-factor, three-level BBD. Similarly, the resultant data were analyzed through "Design-Expert® 11.0 software (Stat-Ease Inc., Minneapolis, Minnesota, USA)" to find analysis of variance, regression equation, and regression coefficients [45]. Results fixed to 2nd order quadratic model and aptness was established by ANOVA, lack of fit and multiple regression coefficients (R^2) values.

Encapsulation efficiency (EE)

Drug encapsulation in micelles is significant for improving the oral bioavailability of CAP [45]. The EE (Y1) of micelles was in an array of 50.38-69.18 %. The polynomial model represents that A and B significantly influence EE.

The quadratic model generated for EE was identified considerably with an F-value of 166.62. The individual variables A, B, interactive term (AB), and quadratic terms A^2 and B^2 significantly influenced EE, P value less than 0.05. "Lack of Fit F-value" (3.49) proposes that it is insignificant. The factorial equation for EE indicated the influence of A is more momentous than B with a good correlation coefficient (R^2) and adjusted R^2 for the model 0.98697 and 0.98104, respectively.

As the dialysis time (A) increased from 60 to 120 min, the EE increased (from 50.38 to 69.18%). At lower points of A, EE escalated from 50.38 to 57.34 %. It clearly indicates that EE decreased from 61.12 to 54.34 % at higher levels of A. As the ratio of the organic phase to the aqueous phase (B) increases from 1 to 2, the EE increases from 50.38 to 69.18 %. At lower points of B, EE escalated from 50.38 to 64.28 %. Inclined points of B show an antagonistic quadratic effect. At inclined levels of B, EE decreased from 65.48 to 54.34 %. Perturbation, 3D surface, and contour plots were constructed to show independent parameters' significant and collective influence on EE. Individual influences of A and B on EE were presented by perturbation plot. Fig. 4(a) shows that A has the most critical consequence on EE, followed by B with a modest outcome. The collective influence of A and B (AB) at a steady level of C on EE is depicted in fig. 4(b) and 4(c). Y1 for all batches was found to be in the range of 50.38-69.18%.

Particle size

Particle size is a significant quality control assessment for nano-micelle. Size distribution is a significant factor concerning micelles' physical properties and stability. The size of a nano-carrier is a crucial aspect that impacts permeation and retention through different cancer tissues and related organs [46]. The particle size of micelles was within an array of 156.46 to 333.94 nm. The polynomial model depicts that all parameters considerably influence micelle particle size.

The quadratic model was significant, having an F-value of 8510.91. Individual variables (A, B and C), interactive term (BC), and quadratic terms A^2 and B^2 were found to have a significant influence on particle size ($P<0.05$). "Lack of Fit F-value" (0.42) proposes that it is not momentous. There is an 81.72 % possibility that a "Lack of Fit F-value" this big could happen due to noise. The factorial equation for particle size indicated that the influence of C is more significant than A and B with a good correlation coefficient (R^2) and adjusted R^2 for the model 0.99749 and 0.99554, respectively.

As the A increases from 60 to 120 min, Y2 inclined (178.12 to 333.94 nm). Y2 readings tended to be higher at lower concentrations of A (178.12 to 312.46 nm). Particle size was reduced with greater concentrations of A (297.79 to 156.46 nm). As the ratio of the organic phase to the aqueous phase (B) increases from 1 to 2, particle size also inclined (182.76 to 312.46 nm). At lower amounts of B, particle size values inclined from 182.76 to 333.94 nm. At higher amounts of B, particle size decreased (299.21 to 186.94 nm). As C increases from 30 to 90 min, the particle size is reduced from 333.94 to 156.46 nm. At lower amounts of C, Y2 declined from 333.94 to 297.79 nm. Similarly, at higher amounts of C, Y2 declined to 156.46 nm. Independent influences of A, B, and C concerning particle size were presented in the perturbation plot. Fig. 5(a) shows that C significantly influences particle size, and B and A have minimal influence. The collective and quadratic effects of independent variables were explicated by 3D response surface and contour plots. The interactive result of A and B at a steady stage of C on PS is presented in fig. 5(b) and 5(c). The interactive impact of B and C (BC) at a steady stage of A on PS is presented in fig. 5(d) and 5(e) and it ranges from156.46-333.94 nm (Y2).

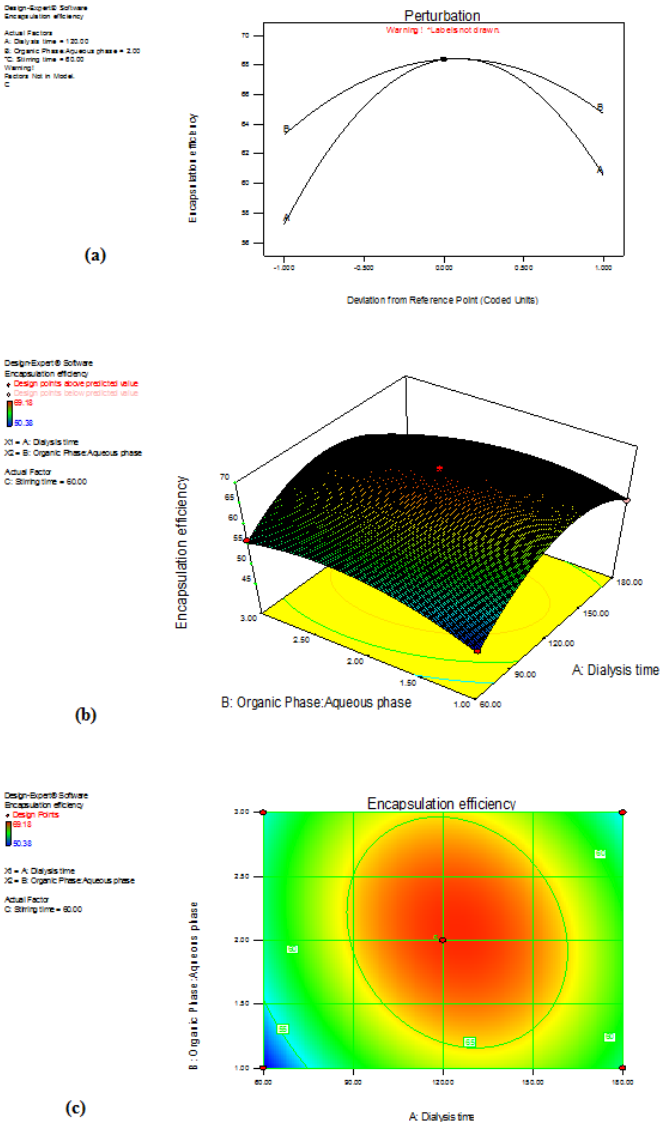

Fig. 4(a): 2D Perturbation plot-effect of A and B on EE; 4(b): 3D-response surface graph presenting the interactive effect of A and B on EE at a steady level of C; 4(c): Contour graph presenting the interactive effect of A and B on EE at a steady level of C

Table 4: Optimal setting acquired by restricting response parameters

Independent variables	Optimized values	Predicted values		Batch	Actual values			
		EE (Y1) %	Particle size (Y2) nm		Encapsulation efficiency (Y1) %	Particle size (Y2) nm	ZP (mV)*	Polydispersity index*
Dialysis time	126 min	67.85	167.54	F1	66.26	170.14±9.2	25.93±2.02	0.26±0.005
Organic phase: Aqueous phase	2.01			F2	67.54	169.37±7.86	24.40±1.38	0.32±0.005
Stirring time	95 min			F3	68.13	168.62±7.12	27.92±5.81	0.18±0.005

*Data are given as mean±standard deviation, n=3

Characterization and evaluation of micelles

EE, particle size, zeta potential, and polydispersity index

The results of EE, particle size, zeta potential, and polydispersity index values are shown in table 4. The EE micelle was satisfactory. The particle size of micelles was similar with lower polydispersity indices. Higher zeta potential values represent increased storage stability of micelles [47].

Surface morphology

The surface morphology of prepared micelles were examined at a magnification of 45000× by TEM. TEM image revealed the well-formed spherical and uniform-sized micelles in a size array of 150-200 nm (fig. 6).

^{1}H NMR and FTIR

The structures of the CAP and polymers were established using ^{1}H NMR and FTIR. Fig. 7(a) shows ^{1}H NMR spectra of CAP, CS, SA, GA-CS-g-SA and CAP-GA-CS-g-SA. Spectra of GA-CS-g-SA presented a pointed signal at d=1.0 ppm; this was endorsed for–CH_2–of SA. The chemical shift of 0.9 ppm and 1.0 ppm could be credited to the–CH_3 hydrogen and methylene hydrogen of the stearate group, respectively. Thus, it has understood that SA was productively grafted to CS [46]. Similarly, the spectra of GA-CS-g-SA indicated

added signal at d=3.5-3.65 ppm belonging to GA. From this, it is apparent how SA and GA functionally joined CS. ^{1}H NMR spectra of CAP shows distinguishing peaks at 0.90 and 1.31 ppm attributed to –CH3 and–CH2– protons of CAP, respectively. All distinguishing peaks of CAP disappeared in both the polymer conjugates, indicating drug encapsulation in the hydrophobic core of the micelle [23].

Fig. 7(b) shows the FTIR spectra of drug, polymer and formulation (CAP, CS, SA, GA-CS-G-SA, and CAP-GA-CS-g-SA). The characteristic signals of amide bands I and II of CS were shifted to 1640 cm^{-1} and 1560 cm^{-1}in spectra of grafted polymer, indicating the amide band between CS and SA. The absorption band of–COOH groups of GA (1706 cm^{-1}) disappeared in the FTIR spectrum of GA-CS-g-SA, indicating the formation of the amide bond between–COOH (GA) and the–NH_2 (CS) groups. The disappearance of prominent peaks of CAP indicates internalization within the hydrophobic core of the polymer [10].

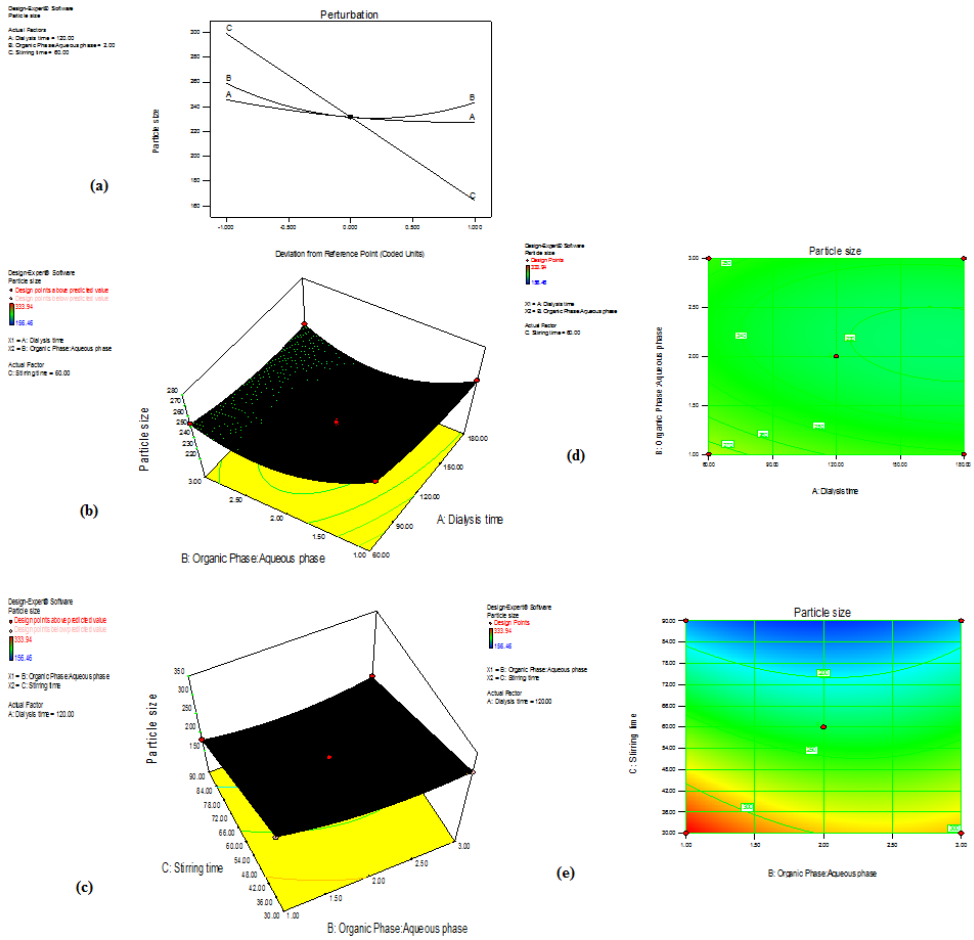

Fig. 5(a): 2D perturbation scheme–influence of A, B, and C on PS(Y2); 5(b): 3D-response surface graph presenting the interactive influence of A and B on Y2 at a C steady level; 5(c): 3D-response surface graph presenting the interactive influence of B and C on Y2 at a steady level of A; 5(d): Contour graph showing the interactive impact of A and B on PS at a C steady level; 5(e): Contour graph showing the interactive impact of B and C on PS at A steady level

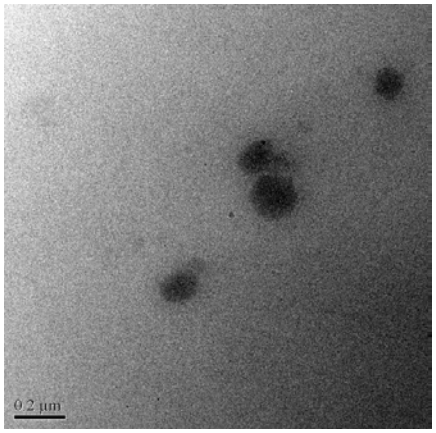

Fig. 6: TEM image of CAP-loaded micelle (45000× magnification)

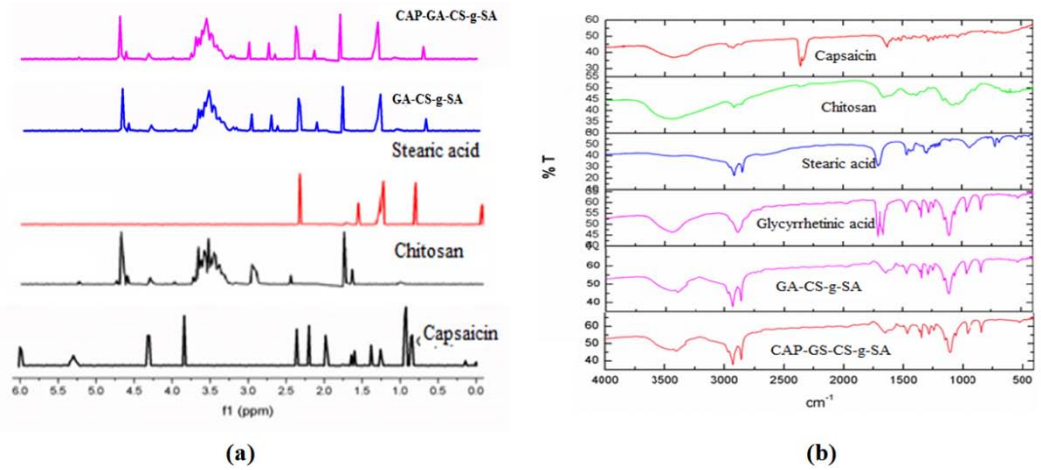

(a) **(b)**

Fig. 7(a):^{1}H NMR spectra of CAP, CS, SA, GA-CS-g-SA and CAP-GA-CS-g-SA; 7(b): FTIR spectra of CAP, CS, SA, GA-CS-g-SA and CAP-GA-CS-g-SA
Note: CAP-Capsaicin; CS-Chitosan; SA-Stearic acid; GA-Glycyrrhetinic acid

XRD and DSC

The free CAP and freeze-dried products of CAP-GA-CS-g-SA micelles were examined in solid state by XRD and DSC. XRD markings of samples are depicted in fig. 8(a). The diffraction peaks of CAP explain the crystalline character, whereas the disappearance of these peaks confirms the freeze-dried micelles' products and the latest solid state [48].

The DSC curve of CAP presents an endothermic peak (67.1 °C), noting the melting point. GA-CS-g-SA's DSC curve has not shown any characteristic endothermic peak, indicating the formation of a more stable complex polymer. The melting peak of CAP nearly disappeared, depicting interaction with the polymer conjugates. Results indicated an exhaustive interaction of CAP and polymers existed in freeze-dried products (fig. 8b).

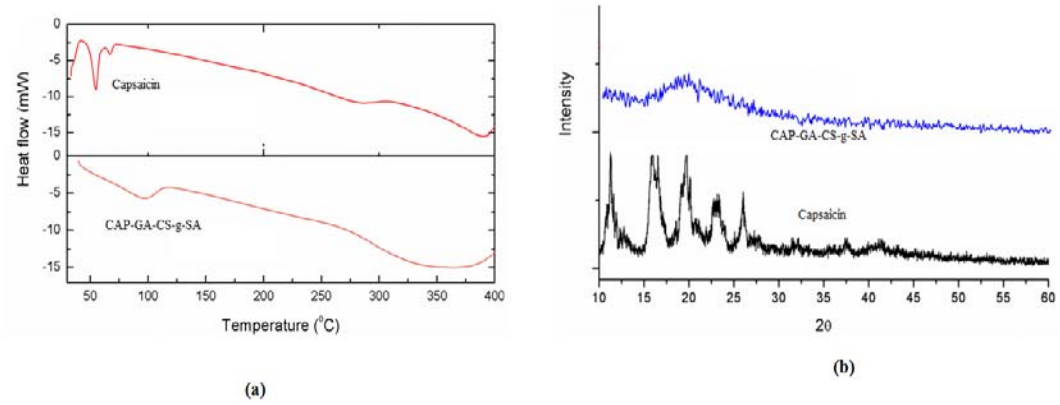

(a) **(b)**

Fig. 8(a): X-ray diffraction patterns of CAP and CAP-GA-SA-g-CS; 8(b): DSC curve of CAP and CAP-GA-SA-g-CS

Hemolysis test

Non-toxicity of the formulation is a compulsory requirement; hence hemolytic performance was determined to identify the safety and biocompatibility of GA-CS-g-SA and CAP-GA-CS-g-SA micelles [33, 50]. Fig. 9 shows the hemolytic activity of plain and drug-loaded micelles. Plain micelles' aqueous suspensions (5 mg/ml) were non-hemolytic. Drug-embedded micelles showed a safe outline with erythrocytes [39]. Optical microscopic images at 400x magnification presented the existence of erythrocytes with plain and drug-loaded micelle, thus proving their intactness and safety [49].

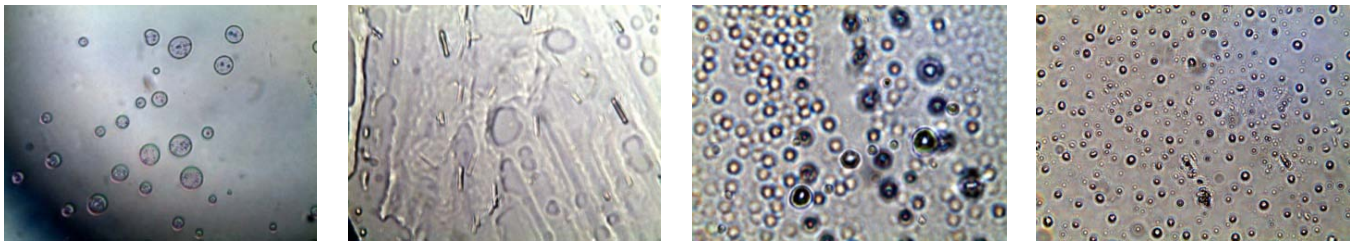

(a) **(b)** **(c)** **(d)**

Fig. 9: Erythrocytes photomicrographs treated with 11(a) PBS; 11(b) SLS; 11(c) GA-CS-g-SA; 11 (d) CAP-GA-CS-g-SA (400x magnification)

In vitro drug release

The drug release performance could distress its pharmacokinetic properties [51]. CAP release from micelles was examined using the dialysis method. Cumulative release plots were constructed, as shown in fig. 10. Nearly 50% of the free CAP was released within 2 h and almost entirely released during 6 h (99.48±2.56%). CAP release from drug-loaded micelles showed a slower and sustained release pattern (86.78% till 24h). The amphiphilic micelle provides physical and chemical stability. It delivers drugs in a controlled manner, and CAP release through the micelle core and penetration from the layer leads to slower release [10, 22, 52].

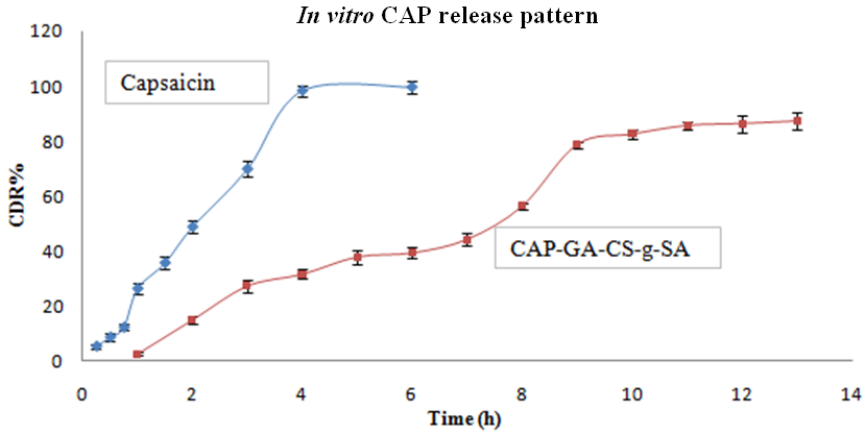

Fig. 10: *In vitro* drug dissolution pattern

Table 5: Stability studies of micelle

Temperature (°C)	Time (days)	Encapsulation efficiency (%)	Particle size (nm)	Polydispersity index (PdI)
4±1 °C	0	68.39±1.13	166.54±6.72	0.192±0.005
	15	67.99±2.12	169.22±4.88	0.182±0.005
	30	68.42±0.96	174.33±3.94	0.224±0.005
	45	67.12±0.6	169.33±2.4	0.214±0.05
	60	68.62±1.06	174.2±3.25	0.184±0.005
	90	68.34±1.16	171.9±3.8	0.181±0.005
25±2 °C	0	68.39±1.13	166.54±6.72	0.192±0.005
	15	68.12±1.76	170.22±4.88	0.182±0.005
	30	67.88±1.92	174.33±3.94	0.224±0.005
	45	66.12±0.6	167.32±2.1	0.254±0.05
	60	67.62±1.6	175.2±3.15	0.185±0.005
	90	68.31±1.26	173.9±3.58	0.180±0.005
40±2 °C	0	68.39±1.13	166.54±6.72	0.192±0.005
	15	67.72±0.88	171.12±1.84	0.236±0.005
	30	68.12±2.06	176.34±2.12	0.188±0.005
	45	68.14±0.16	168.33±2.3	0.234±0.005
	60	68.68±1.06	164.92±3.15	0.187±0.005
	90	68.34±1.09	172.0±3.8	0.185±0.005

Data are given as mean±standard deviation, n=3

Drug release kinetics

Drug release information for developed micelles was built into various kinetic equations to identify order and CAP release patterns [40]. The data obtained shows that the regression coefficient value is near unity for first-order kinetics. Hence it is discussed that the dissolution rate is positively proportional to the drug concentration [41]. Also, the conversion of the dissolution study results into mathematical modelling, such as Higuchi and Korsmeyer-Peppas plots, which suggests the chance of comprehending the drug release strategy. The regression coefficient result is close to one for the Higuchi model, indicating the liberation of the drugs from the matrix (insoluble) as a square root of time (Fickian diffusion Equation) [51].

Stability of micelles

The storage stability of optimized CAP-loaded micelles was examined at various temperatures (4, 25, and 40 °C) for three months. Data of drug content, EE, and particle size of CAP micelles at the 0th, 15th, 30th, 45th, 60th, and 90th day were presented in table 5. At all temperatures, no discernible change in drug amount was found. The EE barely changed between 4 °C and 25 °C, indicating that micelles might protect CAP against deterioration or degradation [11]. At higher temperatures, the EE dramatically decreased, indicating that the micelle structure was being disrupted [47]. Mean particle size steadily inclined along the storage period, which might be related to the dynamic micellar disassembly and re-aggregation to produce a comparatively established system. The average particle size increased over the storage period [23]. Stability experiments show that polydispersity index readings of CAP micelles were below 0.3, indicating the uniform size allocation.

CONCLUSION

In this study, we synthesized GA-CS-g-SA and prepared polymeric micelles by optimizing the process parameters with the aid of BBD. QbD was productively functional for CAP-loaded polymeric micelles development. The main component affecting particle size was stirring speed, whereas reaction time and temperature influenced EE%. The successful grafting of CAP-GA-CS-g-SA was validated by FTIR, NMR, XRD, and DSC measurements. The hemolysis test has proven that the micelles were biocompatible. CAP-loaded GA-CS-g-

SA micelles could increase the solubility and control the release of CAP from the micellar system. The present study is further planned to perform *in vivo* studies to conclude the targeted delivery of CAP into hepatic cells.

ACKNOWLEDGMENT

The authors thank GITAM School of Pharmacy, GITAM Deemed to be University, Hyderabad, for their continuous support in encouraging, motivating, and providing "Design-Expert® 13.0 software (Stat-Ease Inc., Minneapolis, MN, USA)".

FUNDING

This research has no external funding.

AUTHORS CONTRIBUTIONS

The research work and writing were completed by M. K. and reviewed and edited by S. S. Both authors agree with the submission and publication. Both have read and agreed to the published edition of the manuscript.

CONFLICTS OF INTERESTS

Declared none

REFERENCES

1. Hughes E, Hopkins LJ, Parker R. Survival from alcoholic hepatitis has not improved over time. PLOS ONE. 2018 Feb;13(2):e0192393. doi: 10.1371/journal.pone.0192393, PMID 29444123.
2. Mitra S, De A, Chowdhury A. Epidemiology of non-alcoholic and alcoholic fatty liver diseases. Transl Gastroenterol Hepatol. 2020 Apr;5:16. doi: 10.21037/tgh.2019.09.08, PMID 32258520.
3. Singal AK, Louvet A, Shah VH, Kamath PS. Grand rounds: alcoholic hepatitis. J Hepatol. 2018 Jun;69(2):534-43. doi: 10.1016/j.jhep.2018.05.001, PMID 29753761.
4. Gao B, Bataller R. Alcoholic liver disease: pathogenesis and new therapeutic targets. Gastroenterology. 2011 Sep;141(5):1572-85. doi: 10.1053/j.gastro.2011.09.002, PMID 21920463.
5. Sukmanadi M, Effendi MH. The protective effect of capsaicin (Capsicum annum l) against the induction of aflatoxin b1 in hepatocytes: A study of liver histopathology in mice (mus musculus). Res J Pharm Technol. 2021 Feb;14(2):813-6. doi: 10.5958/0974-360X.2021.00143.8.
6. Koneru M, Sahu BD, Mir SM, Ravuri HGora, Kuncha M, Mahesh Kumar JM. Capsaicin, the pungent principle of peppers, ameliorates alcohol-induced acute liver injury in mice via modulation of matrix metalloproteinases. Can J Physiol Pharmacol. 2018 Apr;96(4):419-27. doi: 10.1139/cjpp-2017-0473, PMID 29053935.
7. Baranidharan G, Das S, Bhaskar A. A review of the high-concentration capsaicin patch and experience in its use in the management of neuropathic pain. Ther Adv Neurol Disord. 2013 Sep;6(5):287-97. doi: 10.1177/1756285613496862, PMID 23997814.
8. Rollyson WD, Stover CA, Brown KC, Perry HE, Stevenson CD, McNees CA. Bioavailability of capsaicin and its implications for drug delivery. J Control Release. 2014 Dec;196:96-105. doi: 10.1016/j.jconrel.2014.09.027, PMID 25307998.
9. Mateescu MA, Ispas Szabo P, Assaad E. Chitosan and its derivatives as self-assembled systems for drug delivery. Control Drug Deliv. 2015:85-125.
10. Song P, Lu Z, Jiang Tianze, Han W, Chen X, Zhao X. Chitosan coated pH/redox-responsive hyaluronic acid micelles for enhanced tumor-targeted co-delivery of doxorubicin and siPD-L1. Int J Biol Macromol. 2022 Sep;222(A):1078-91. doi: 10.1016/j.ijbiomac.2022.09.245, PMID 36183754.
11. Jiang X, Ma M, Li M, Shao S, Yuan H, Hu F. Preparation and evaluation of novel emodin-loaded stearic acid-g-chitosan oligosaccharide nanomicelles. Nanoscale Res Lett. 2020 Apr;15(1):93. doi: 10.1186/s11671-020-03304-1, PMID 32335740.
12. Wang XH, Tian Q, Wang W, Zhang CN, Wang P, Yuan Z. *In vitro* evaluation of polymeric micelles based on hydrophobically-modified sulfated chitosan as a carrier of doxorubicin. J Mater Sci Mater Med. 2012 Apr;23(7):1663-74. doi: 10.1007/s10856-012-4627-1, PMID 22538726.
13. Lallemand B, Gelbcke M, Dubois J, Prevost M, Jabin I, Kiss R. Structure-activity relationship analyses of glycyrrhetinic acid derivatives as anticancer agents. Mini Rev Med Chem. 2011 Sep 1;11(10):881-7. doi: 10.2174/138955711796575443, PMID 21762107.
14. Huang W, Wang W, Wang P, Zhang CN, Tian Q, Zhang Y. Glycyrrhetinic acid-functionalized degradable micelles as liver-targeted drug carrier. J Mater Sci Mater Med. 2011 Apr 1;22(4):853-63. doi: 10.1007/s10856-011-4262-2, PMID 21373811.
15. Tye H. Application of statistical 'design of experiments' methods in drug discovery. Drug Discov Today. 2004 Jun 1;9(11):485-91. doi: 10.1016/S1359-6446(04)03086-7, PMID 15149624.
16. Alafaghani A, Qattawi A. Investigating the effect of fused deposition modeling processing parameters using Taguchi design of experiment method. J Manuf Processes. 2018;36:164-74. doi: 10.1016/j.jmapro.2018.09.025.
17. Krishna PM. Anchakishore Babu, Palanatimamatha. Formulation and optimization of ceritinib loaded nanobubbles by box-behnken design. Int J Appl Pharm. 2022 Jul;14(4):219-26.
18. Singh B, Kapil R, Nandi M, Ahuja N. Developing oral drug delivery systems using formulation by design: vital precepts, retrospect and prospects. Expert Opin Drug Deliv. 2011 Oct;8(10):1341-60. doi: 10.1517/17425247.2011.605120, PMID 21790511.
19. Kan S, Lu J, Liu J, Wang J, Zhao Y. A quality by design (QbD) case study on enteric-coated pellets: screening of critical variables and establishment of design space at laboratory scale. Asian J Pharm Sci. 2014 Oct;9(5):268-78. doi: 10.1016/j.ajps.2014.07.005.
20. N Politis S, Colombo P, Colombo G, M Rekkas D. Design of experiments (DoE) in pharmaceutical development. Drug Dev Ind Pharm. 2017 Jun;43(6):889-901. doi: 10.1080/03639045.2017.1291672, PMID 28166428.
21. Cheng M, Gao X, Wang Y, Chen H, He B, Xu H. Synthesis of glycyrrhetinic acid-modified chitosan 5-fluorouracil nanoparticles and its inhibition of liver cancer characteristics *in vitro* and *in vivo*. Mar Drugs. 2013 Sep;11(9):3517-36. doi: 10.3390/md11093517, PMID 24048270.
22. Lia X, Youb J, FudeCuia Y, Dub, hong Yuanb, Fuqiang Hub. Preparation and characteristics of SA grafted CS oligosaccharide polymeric micelle containing 10-hydroxy camptothecin. Asian J Pharm Sci. 2008 Feb;3(2):80-7.
23. Chen Q, Sun Y, Wang J, Yan G, Cui Z, Yin H. Preparation and characterization of glycyrrhetinic acid-modified stearic acid-grafted chitosan micelles. Artif Cells Nanomed Biotechnol. 2015;43(4):217-23. doi: 10.3109/21691401.2013.845570, PMID 24093764.
24. Xu W, Cui Y, Ling P, Li LB. Preparation and evaluation of folate-modified cationic pluronic micelles for a poorly soluble anticancer drug. Drug Deliv. 2012;19(4):208-19. doi: 10.3109/10717544.2012.690005, PMID 22643055.
25. Hu FQ, Ren GF, Yuan H, Du YZ, Zeng S. Shell cross-linked stearic acid grafted chitosan oligosaccharide self-aggregated micelles for controlled release of paclitaxel. Colloids Surf B Biointerfaces. 2006 Jul;50(2):97-103. doi: 10.1016/j.colsurfb.2006.04.009, PMID 16759840.
26. Zhu QL, Zhou Y, Guan M, Zhou XF, Yang SD, Liu Y. Low-density lipoprotein-coupled N-succinyl chitosan nanoparticles co-delivering siRNA and doxorubicin for hepatocyte-targeted therapy. Biomaterials. 2014 Jul;35(22):5965-76. doi: 10.1016/j.biomaterials.2014.03.088, PMID 24768047.
27. Patra A, Satpathy S, Shenoy AK, Bush JA, Kazi M, Hussain MD. Formulation and evaluation of mixed polymeric micelles of quercetin for treatment of breast, ovarian, and multidrug-resistant cancers. Int J Nanomedicine. 2018;13:2869-81. doi: 10.2147/IJN.S153094, PMID 29844670.
28. Salimi A, Sharif Makhmal Zadeh B, Kazemi M. Preparation and optimization of polymeric micelles as an oral drug delivery system for deferoxamine mesylate: *in vitro* and ex vivo studies. Res Pharm Sci. 2019 Aug;14(4):293-307. doi: 10.4103/1735-5362.263554, PMID 31516506.

29. Dash S, Murthy PN, Nath L, Chowdhury P. Kinetic modeling on drug release from controlled drug delivery systems. Acta Pol Pharm. 2010 May;67(3):217-23. PMID 20524422.
30. Kemkar K, Sathiyanarayanan A, Mahadik K. 6-shogaol rich ginger oleoresin loaded mixed micelles enhances *in vitro* cytotoxicity on mcf-7 cells and *in vivo* anticancer activity against dal cells. Int J Pharm Pharm Sci. 2018 Jan;10(1):160-8. doi: 10.22159/ijpps.2018v10i1.23077.
31. An JY, Yang HS, Park NR, Koo TS, Shin B, Lee EH. Development of polymeric micelles of oleanolic acid and evaluation of their clinical efficacy. Nanoscale Res Lett. 2020;15(1):133. doi: 10.1186/s11671-020-03348-3, PMID 32572634.
32. Zhou YY, Du YZ, Wang L, Yuan H, Zhou JP, Hu FQ. Preparation and pharmacodynamics of stearic acid and poly (lactic-co-glycolic acid) grafted chitosan oligosaccharide micelles for 10-hydroxy camptothecin. Int J Pharm. 2010 Jun;393(1-2):143-51. doi: 10.1016/j.ijpharm.2010.04.025, PMID 20420886.
33. Dou J, Zhang H, Liu X, Zhang M, Zhai G. Preparation and evaluation *in vitro* and *in vivo* of docetaxel loaded mixed micelles for oral administration. Colloids Surf B Biointerfaces. 2014;114:20-7. doi: 10.1016/j.colsurfb.2013.09.010, PMID 24157590.
34. Darandale SS, Vavia PR. Cyclodextrin-based nanosponges of curcumin: formulation and physicochemical characterization. J Incl Phenom Macrocycl Chem. 2013 Apr;75(3-4):315-22. doi: 10.1007/s10847-012-0186-9.
35. Dobrovolskaia MA, Clogston JD, Neun BW, Hall JB, Patri AK, McNeil SE. Method for analysis of nanoparticle hemolytic properties *in vitro*. Nano Lett. 2008 Aug;8(8):2180-7. doi: 10.1021/nl0805615, PMID 18605701.
36. Song Z, Zhu W, Liu N, Yang F, Feng R. Linolenic acid-modified PEG-PCL micelles for curcumin delivery. Int J Pharm. 2014 Aug;471(1-2):312-21. doi: 10.1016/j.ijpharm.2014.05.059, PMID 24939613.
37. Costa P, Sousa Lobo JM. Modeling and comparison of dissolution profiles. Eur J of Pharmaceutical Sciences. 2001 May;13(2):123-33. doi: 10.1016/s0928-0987(01)00095-1, PMID 11297896.
38. Wei H, Xu L, Sun Y, Li G, Cui Z, Yan G. Preliminary pharmacokinetics of PEGpegylated oxaliplatin polylactic acid nanoparticles in rabbits and tumor-bearing mice. Artif Cells Nanomed Biotechnol. 2015 Feb;43(4):258-62. doi: 10.3109/21691401.2014.883402, PMID 24564351.
39. Termsarasab U, Cho HJ, Kim DH, Chong S, Chung SJ, Shim CK, Moon HT, Kim DD. Chitosan oligosaccharide–arachidic acid-based nanoparticles for anti-cancer drug delivery. International Journal of Pharmaceutics. 2013 Jan;441(1-2):373-80. doi: 10.1016/j.ijpharm.2012.11.018, PMID 23174411.
40. Kovacs A, Berko S, Csanyi E, Csoka I. Development of nanostructured lipid carriers containing salicyclic acid for dermal use based on the quality by design method. Eur J Pharm Sci. 2017;99:246-57. doi: 10.1016/j.ejps.2016.12.020, PMID 28012940.
41. Beg S, Saini S, Bandopadhyay S, Katare OP, Singh B. QbD-driven development and evaluation of nanostructured lipid carriers (NLCs) of olmesartan medoxomil employing multivariate statistical techniques. Drug Dev Ind Pharm. 2018 Mar;44(3):407-20. doi: 10.1080/03639045.2017.1395459, PMID 29048242.
42. Patel M, Sawant K. A quality by design concept on lipid-based nanoformulation containing antipsychotic drug: screening design and optimization using response surface methodology. J Nanomed Nanotechnol. 2017 May;8(3):1-11. doi: 10.4172/2157-7439.1000442.
43. Hu FQ, Jiang XH, Huang X, Wu XL, Yuan H, Wei XH, Yong Zhong Du. Enhanced cellular uptake of chlorine e6 mediated by stearic acid–grafted chitosan oligosaccharide micelles. Journal of Drug Targeting. 2009 Jun;17(5):384-91. doi: 10.1080/10611860902894325, PMID 19343607.
44. Nazzal S, Khan MA. Response surface methodology for the optimization of ubiquinone self-nano emulsified drug delivery system. AAPS PharmSciTech. 2002 Jan;3(1):E3. doi: 10.1208/pt030103, PMID 12916956.
45. Wei TK, Manickam S. Response surface methodology, an effective strategy in the optimization of the generation of curcumin-loaded micelles. Asia-Pac J Chem Eng. 2012 Jan;7(Suppl 1):125-33. doi: 10.1002/apj.661.
46. Shaikh MV, Kala M, Nivsarkar M. Formulation and optimization of doxorubicin-loaded polymeric nanoparticles using box-Behnken design: ex-vivo stability and *in vitro* activity. European Journal of Pharmaceutical Sciences. 2017;100:262-72. doi: 10.1016/j.ejps.2017.01.026, PMID 28126560.
47. Abbas G, Hanif M, Khan MA. pH-responsive alginate polymeric rafts for controlled drug release by using box bBehnken response surface design. Designed Monomers and Polymers. 2017 Sep;20(1):1-9. doi: 10.1080/15685551.2016.1231046, PMID 29491774.
48. Du YZ, Cai LL, Li J, Zhao MD, Chen FY, Yuan H, Fu-Qiang Hu. Receptor-mediated gene delivery by folic acid-modified stearic acid-grafted chitosan micelles. International Journal of Nanomedicine. 2011 Aug;6:1559-68. doi: 10.2147/IJN.S23828, PMID 21845046.
49. Chen Q, Sun Y, Wang J, Yan G, Cui Z, Yin H, Haitian W. Preparation and characterization of glycyrrhetinic acid-modified stearic acid-grafted chitosan micelles. Artificial Cells, Nanomedicine, and Biotechnology. 2015 Oct;43(4):217-23. doi: 10.3109/21691401.2013.845570, PMID 24093764.
50. Chu Y, Sun T, Xie Z, Sun K, Jiang C. Physicochemical characterization and pharmacological evaluation of novel propofol micelles with low-lipid and low-free propofol. Pharmaceutics. 2022 Feb;14(2):414. doi: 10.3390/pharmaceutics14020414, PMID 35214146.
51. Xie YT, Du YZ, Yuan H, Hu FQ. Brain-targeting study of stearic acid–grafted chitosan micelle drug-delivery system. International Journal of Nanomedicine. 2012 Jun;7:3235-44. doi: 10.2147/IJN.S32701, PMID 22802685.
52. Mohanty AK, Mohanta GP. Dual anticancer drug-loaded methoxy poly (ethylene glycol)-poly (ε-caprolactone) block copolymeric micelles as novel drug carriers. International Journal of Pharmacy and Pharmaceutical Sciences. 2014 Sep;6(9):328-32.